Supplementary Appendix

Supplemental Material and Methods

Enzyme Preparation. The mouse recombinant TREX1 enzyme (amino acids 1 -242) was expressed in bacteria and purified as stable homodimers as described (1, 2). Protein concentrations were determined by A_{280} using the molar extinction coefficient for TREX1 protomer ε=23,950 $M^{-1}cm^{-1}$.

Protein Crystallization and X-ray Data Collection. The TREX1 D18N mutant was crystallized using the sitting drop vapor diffusion technique. The protein was dialyzed in 20 mM MES (pH 6.5), 50 mM NaCl and concentrated to 10 mg/mL. The pseudo-palindromic oligonucleotide DNA used for crystallization (5'-TCACGTGCTGACGTCAGCACGACG-3' (Operon)) was self-annealed in buffer consisting of 20 mM NaCl, 5 mM $MgCl_2$, and 5 mM MES, pH 6.5. The complex was formed by incubating dsDNA with the protein in a 1:1 ratio and 5 mM magnesium chloride. A volume of 1 µl protein complex at 4 mg/ml TREX1 was mixed with an equal volume of reservoir solution and placed on a bridge above 500 µl of the reservoir solution. Optimized crystals of the TREX1 D18N mutant grew in 0.1 M sodium acetate and 9% PEG 4000 at 25°C. Prior to data collection all crystals were immersed in reservoir solution containing 10% oil (1:1 mineral oil and pantone-N) in preparation for cryo-cooling. Crystals were mounted on a nylon loop and flash cooled to 100 K in a stream of liquid nitrogen.

Phasing and Refinement. The X-ray data were collected using CuKα radiation on a MicroMax 007 generator and a Saturn 92 CCD detector (Rigaku). Intensity data were processed using the programs d*TREK (3). The TREX1 D18N mutant in complex with dsDNA belongs to the P21 spacegroup (Table S5). Phases for the data were obtained by maximum likelihood molecular replacement using the program PHASER (4) and the TREX1 dimer (PDB ID: 2OA8), including only a single monomer as the search model (protein only). The model was built in the program COOT (5) following composite omit procedures and the structures refined using the programs Refmac5 (6), and Phenix.refine (7). Translation/libration/screw (TLS) refinement was utilized to independently define subgroups and to further refine their directions of movement as individual rigid bodies (8). The inspection of clashes and stereochemical parameters was carried out using

the program PDB_REDO (9). The all-atom clashscore is 4.04 and Ramachandran plot shows 97% residues in favored regions and 3% in allowed regions. All structure figures were generated in the program Pymol (Schrödinger, LLC).

Animals. *TREX1* D18N mutant mice were generated on a 129S6/SvEvTac background using an allelic replacement strategy as shown in Fig. S3 (Taconic, NY, USA). Briefly, the *TREX1* D18N targeting vector was modified by site directed mutagenesis. Embryonic stem cell clones that underwent homologous recombination were selected for expression of the NEO cassette and screened for expression of the mutant allele. Positive D18N clones were expanded and injected into blastocysts. Chimeric mice were bred to Cre deleters to remove the NEO cassette. Transmission of the *TREX1* D18N allele was confirmed by sequencing of tail DNA. Males and females exhibited a similar phenotype, so both sexes were used in these studies. All experiments were performed in accordance with the guidelines set forth by the Institutional Animal Care and Use Committee at Wake Forest Baptist Medical Center.

Genotyping. 1-2 mm tail snips were collected from weanling mice. Genomic DNA was isolated according to the DNeasy kit (Qiagen, MD, USA) protocol and the *TREX1* gene was amplified using the following primers:
5’ CCTGCTGCTACTCATTACCCCATC 3’
3’ AGGAGAGAGGGACTGTACCTCATCC 5’
OneTaq® DNA Polymerase (New England Biolabs, MA, USA) was used for DNA amplification. Thermocycler conditions were as follows: 94°C 3 min, (94°C 30 sec, 54°C 20 sec, 68°C 90 sec) x 35 cycles. PCR products were resolved on a 1% agarose gel. Bands of the appropriate size (1KB) were excised and DNA was extracted using a QIAquick Gel Extraction Kit (Qiagen). Sequencing of gel extracted DNA was performed by Genewiz, Inc (NC, USA) using the following primer:
5’ ACAGCATCGCTGCCCTAAAG 3’ .

Expression of *TREX1* alleles by RT-PCR. The *TREX1* transcript was detected using cDNA prepared from mouse liver total RNA and the following primers:
5’ AGGGACAGGGCAGACCAAGAA 3’

3’ TTACTGCCCAGGTGAGGCCA 5’

Q5® Hot Start High-fidelity 2x Master Mix (New England Biolabs, MA, USA) was used for cDNA amplification. Thermocycler conditions were as follows: 98°C 2 min, (98°C 10 sec, 69°C 20 sec, 72°C 40 sec) x 35 cycles, 72°C 2 min. PCR products were resolved on a 1% agarose gel.

TREX1 protein purification. Thymus, salivary gland, cervical lymph nodes, heart, liver, kidney, spleen, and brain were pooled from 8 WT and 8 *TREX1*$^{D18N/D18N}$ male and female mice. Tissues were stored at -80°C until use and samples were kept on ice or at 4°C throughout the procedure. Tissue pools were suspended in lysis buffer (50 mM Tris pH 8.2, 1 mM DTT, 1 mM EDTA, 10% glycerol, 10 μg/ml BSA, 0.1 M NaCl, and Complete Protease Inhibitor Cocktail (Roche, Basel, Switzerland)) then disrupted using a dounce homogenizer. Homogenates were centrifuged for 20 minutes at 10,000 rpm (12,000 x g). Protamine sulfate (0.12% final concentration) was added to supernatants. Samples were incubated for 5 min then centrifuged for 10 min at 16,000 rpm (30,000 x g). Supernatants were collected and dialyzed overnight against dialysis buffer (50 mM Tris pH 8.2, 1 mM DTT, 1 mM EDTA, 10% glycerol, and 0.1 M NaCl). Dialyzed samples were centrifuged for 30 min at 20,000 rpm (48,000 x g). Supernatants were loaded onto a single-stranded DNA cellulose (Sigma, MO, USA) column that had been equilibrated overnight in dialysis buffer. The column was washed with dialysis buffer containing 10 μg/ml BSA then with the same buffer containing 0.2 M NaCl then 0.5 M NaCl. Bound proteins were step-eluted with buffer containing 2 M NaCl. Fractions collected during wash and elution steps were dialyzed for 3 hours against dialysis buffer. Concentrated samples were used in western blots and diluted samples were used in exonuclease assays.

TREX1 western blot. Proteins were separated by SDS-PAGE than transferred to a nitrocellulose membrane (Life Technologies, CA, USA). Membranes were blocked with TBS containing 0.1% Tween 20 (TBST) and 5% milk powder then incubated overnight at 4°C with polyclonal rabbit α-mouse TREX1 antibody diluted 1:100 in TBST. After washing in TBST, membranes were incubated for 1 hr at room temperature with HRP-conjugated anti-rabbit IgG (GE Healthcare, Buckinghamshire, UK). After washing in TBST, bound secondary antibody was visualized by enhanced chemiluminescence (Western Lightening Plus ECL, PerkinElmer, Inc, MA, USA). For generation of the rabbit α-mouse TREX1 antibody, TREX1 enzyme was

recombinately expressed in *E. coli* and purified by ssDNA cellulose chromatography (10). Polyclonal antibody was generated to purified TREX1 enzyme by Rockland, Inc. (PA, USA).

ssDNA exonuclease assay. The exonuclease assays contained 20 mM Tris pH 7.5, 5 mM $MgCl_2$, 2 mM DTT, 100 μg/ml BSA, 50 nM fluorescein-labeled 30-mer oligonucleotide (Operon, AL, USA), and TREX1 enzyme. Reactions were incubated at 25 °C for 15 min, quenched by the addition of 3 volumes of cold ethanol, and dried *in vacuo*. The reaction products were resuspended in 4 μl of formamide and separated on 23% denaturing polyacrylamide gels. Fluorescently labeled bands were visualized using a Storm PhosphorImager (GE Healthcare, Buckinghamshire, UK).

qPCR. 100 ng/μl cDNA was added to TaqMan Universal PCR Master Mix and TaqMan assay for *TREX1* or *Gapdh*. Reactions were performed using an Applied Biosystems 7500 Real-time PCR system. Data were analyzed using Applied Biosystems 7500 software v2.0.5. The ΔΔCt method was used to normalize *TREX1* expression to *Gapdh* expression. The level of *TREX1* expression in WT liver was set at 1. Data were collected from 3 male and 3 female *TREX1*$^{WT/WT}$ and *TREX1*$^{D18N/D18N}$ mice in two independent experiments.

Histology. Tissues were collected from 3-8 mice of each sex and genotype at multiple time points (3 wks, 2 mo, 4 mo, 6 mo), fixed in 10% neutral buffered formalin for 24-48 hours, decalcified in 0.35 M EDTA if indicated, then processed routinely. Paraffin embedded tissues were sectioned at 5 μm then stained with hematoxylin and eosin (H&E). H&E stained slides were examined and scored by a veterinary pathologist (JLG). Lesions were scored as outlined in Tbls S1-S4.

Immunofluorescence. Tissues were frozen in OCT (Sakura Finetek, CA, USA) then stored at -80°C until sectioning. Tissues were sectioned at 5 μm on a Microm cryostat 525 (Thermo Scientific, MA, USA). Sections warmed to room temperature were fixed for 5 min in ice-cold acetone then washed twice in PBS. Tissues were blocked for 1 hr in PBS containing 1% BSA then washed twice in PBS. Tissues were incubated overnight at 4°C with antibody to mouse IgG

(goat α-mouse IgG Alexa Fluor 488, Abcam) diluted 1:1000 in PBS. Tissues were washed three times in PBS then were mounted with Fluoroshield Mounting Medium with DAPI (Abcam).

Flow cytometry. Spleens collected in two independent experiments from 8 total 4-5 month old female mice of each genotype were mechanically disrupted on a wire mesh screen into RPMI 1640 (Hyclone, UT, USA) supplemented with 10% heat-inactivated FCS (Hyclone), L-glutamine (Hyclone), penicillin-streptomycin (Cellgro, VA, USA), and β-mercaptoethanol (Gibco, NY, USA) (cRPMI). Red blood cells were lysed for 1 minute in ACK buffer (Lonza, Basel, Switzerland). Samples were resuspended in cRPMI and cell counts were performed by hemocytometer. For surface staining, samples were incubated with antibody diluted 1:100 in PBS with 2% FCS for 1 hr at 4°C. For T regulatory cell enumeration, cells were treated according to the Mouse T Regulatory Cell Staining Kit (E Biosciences, CA, USA) protocol. Samples were acquired on a CANTO II instrument (BD Biosciences, CA, USA) and data were analyzed using FloJo software (TreeStar, OR, USA). The following antibodies (all from BD Biosciences) were used for surface staining: rat α-mouse CD4-PE, rat α-mouse CD8-PerCP, rat α-mouse B220-APC, rat α-mouse CD138-PE, rat α-mouse CD69-FITC, rat α-mouse CD62L-AP-Cy7.

Statistical analysis. Data were expresses as the mean ± SEM. Student's t-test was used to compare two independent data sets. Two-way ANOVA was used for multiple comparisons. Differences between groups were determined to be significant when $p < 0.05$. All statistical analyses were performed using SigmaPlot 12.5 software (CA, USA).

Supplemental Figures

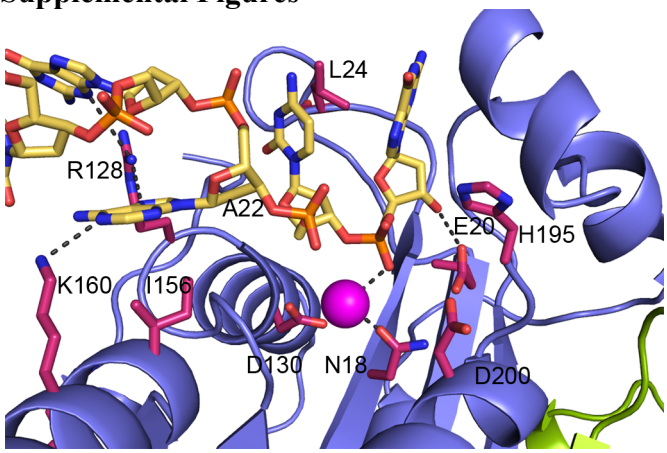

Fig. S1. TREX1 D18N active site tightly binds the substrate strand of unwound dsDNA. The D18N mutation results in active site coordination of only one of the two Mg^{2+} ions (magenta) required for catalysis. The extensive protein-dsDNA interactions coupled with the catalytic inactivity of the D18N mutant traps dsDNA in the active site.

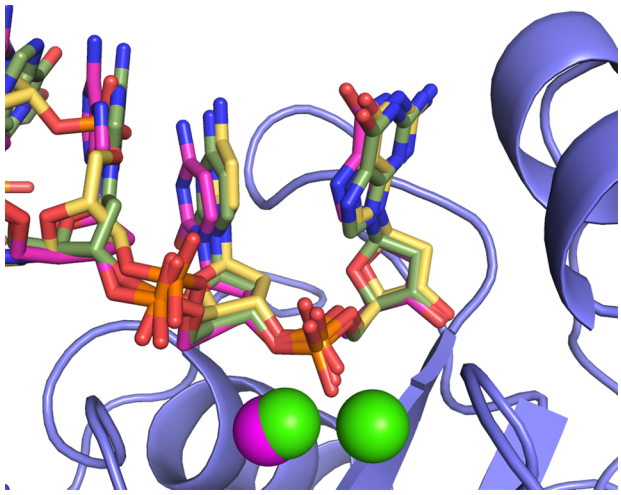

Fig. S2. Terminal nucleotide binding in the TREX1 active site. A superposition of the TREX1 tight (yellow) and loose (green) complexes onto a TREX1-ssDNA complex (magenta, pdbid: 2OA8 [10]) shows the terminal two nucleotides on the substrate strands of the dsDNA complexes are positioned correctly in the active site. Only a single TREX1 is shown for clarity. The single magnesium ion is shown in magenta and the two calcium ions in the ssDNA complex are shown in green.

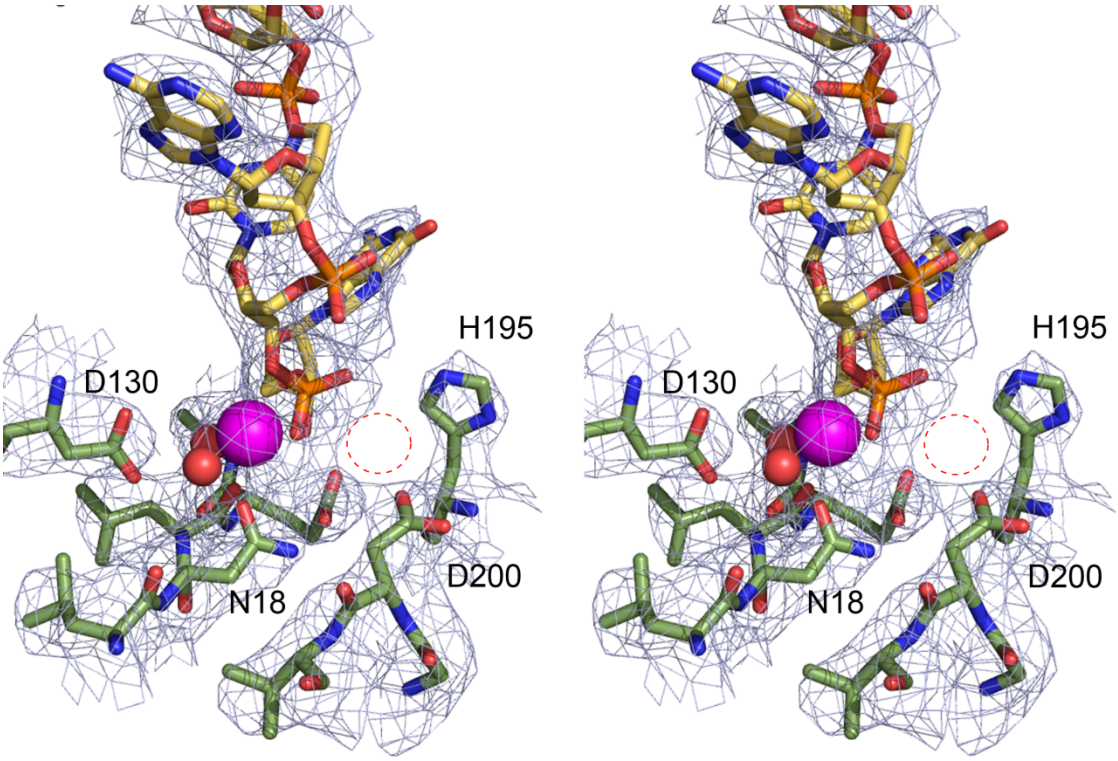

Fig. S3. Electron density in TREX1 active site. Stereo image of $2F_o$-F_c electron density (1σ) shown around the DNA (yellow sticks), Mg ion (magenta) and water molecules (orange) in the active site of TREX1 D18N (green sticks). The density reveals only a single Mg ion in the active site of the TREX1 D18N mutant protein. The position of the missing Mg necessary for catalysis is indicated by the dashed circle. The electron density was calculated with a simulated annealing composite omit procedure using the final refined model.

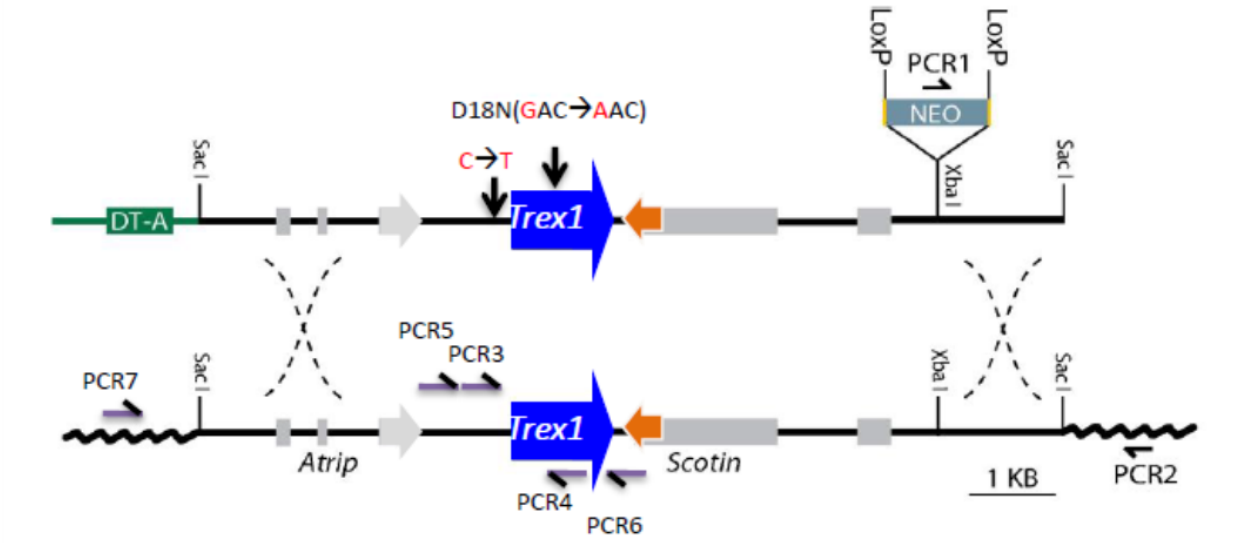

Fig. S4. Replacement of the *TREX1* WT allele with the *TREX1* D18N allele. The R1 129 mouse *TREX1* genomic region (~10kb) flanked by SacI sites (*lower*) and the vector used for targeted homologous recombination (*upper*) are shown (Boxes, exons; lines, introns; squiggle lines, mouse genomic sequences flanking the region of homology; D18N codon, point mutation introduced into the vector *TREX1* coding exon and C→T change in *TREX1* 5'UTR; NEO, neomycin resistance gene; DT-A^{-}, diphtheria toxin A gene; LoxP, recognition site for Cre recombinase; PCR1-7, PCR primers). The linearized *TREX1* D18N vector was electroporated into XSV1 ES cells (of a 129S6/SvEvTac origin) and DT-A^{-} G418-resistant colonies were selected for screening using PCR1/PCR2 and PCR3/PCR4 to identify candidate ES cell clones for targeted homologous recombination. Both PCR3 and PCR4 contain a 3' terminal mispair unless the ES clone contains the targeted *TREX1* D18N mutant allele. PCR positive clones for both reactions with the expected size PCR products had integrated the NEO linked vector into the *TREX1* locus. A third PCR using PCR5/PCR6 recovers a 1.4 kb genomic fragment and sequencing confirmed targeting of the *Trex1* mutant allele and the appropriate heterozygosity corresponding to the presence of both the WT and mutant alleles in the ES cell clones. Positive D18N ES clones were expanded, mouse C57BL/6NTac blastocysts were injected, chimeric mice were generated, and germline transmission of the *TREX1* D18N allele from chimeras was confirmed by sequencing of tail DNA. Chimeras were bred to 129-Tg(Prm-Cre)58Og/J mice (Jackson Laboratory). The transgene in this strain is comprised of the mouse protamine 1

promoter and the Cre recombinase coding sequence and mediate the efficient recombination of a Cre target transgene in the male germ line, but not in other tissues; therefore two rounds of breeding were used: breeding of chimeras to the Cre-deleter females (N1 generation) and then – their heterozygous male progeny to 129SvEvTac females (N2 generation). Cre deletion of the NEO cassette was confirmed by PCR.

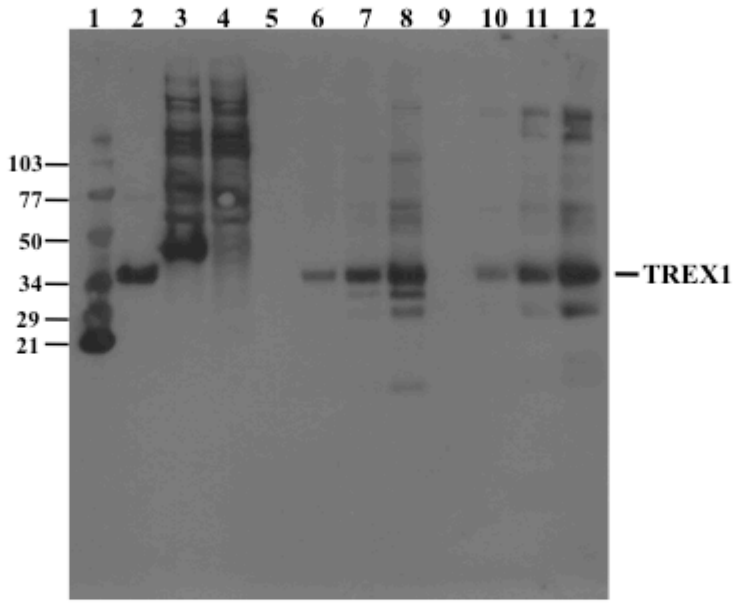

Fig. S5 Endogenous TREX1 D18N protein. Extracts were prepared from *TREX1* WT and *TREX1*$^{D18N/D18N}$ mouse tissues and loaded onto separate ssDNA-cellulose columns, washed, and eluted proteins were fractionated by SDS-PAGE. TREX1 protein was detected by immunoblotting as described above in this Supplementary Appendix. Lane 1, Bio-Rad mol. wt. prestained standards; Lane 2, pure recombinant mouse TREX1 1-242 (24ng) (1); Lane 3, HEK 293T whole cell lysate transfected with pEBB-TREX1 (1–314) N-HA (N terminal HA tag) (11); Lane 4, HEK 293T whole cell lysate transfected with empty pEBB plasmid; Lane 5, blank; Lanes 6-8, increased amounts of ssDNA cellulose elution from mouse TREX1 WT sample; Lane 9, blank; and Lanes 10-12, increased amounts of ssDNA cellulose elution from mouse TREX1 D18N sample.

The band indicated as TREX1 was confirmed by mass spec analysis. Protein eluted from the ssDNA cellulose column and the same mol. wt. standards (Lanes 1-4) were fractionated by

SDS-PAGE and stained with Coomassie Blue. The region of the lane predicted to contain the mouse TREX1 D18N protein, as determined by the size standards, was excised and the TREX1 D18N protein was detected in the sample by mass spec analysis.

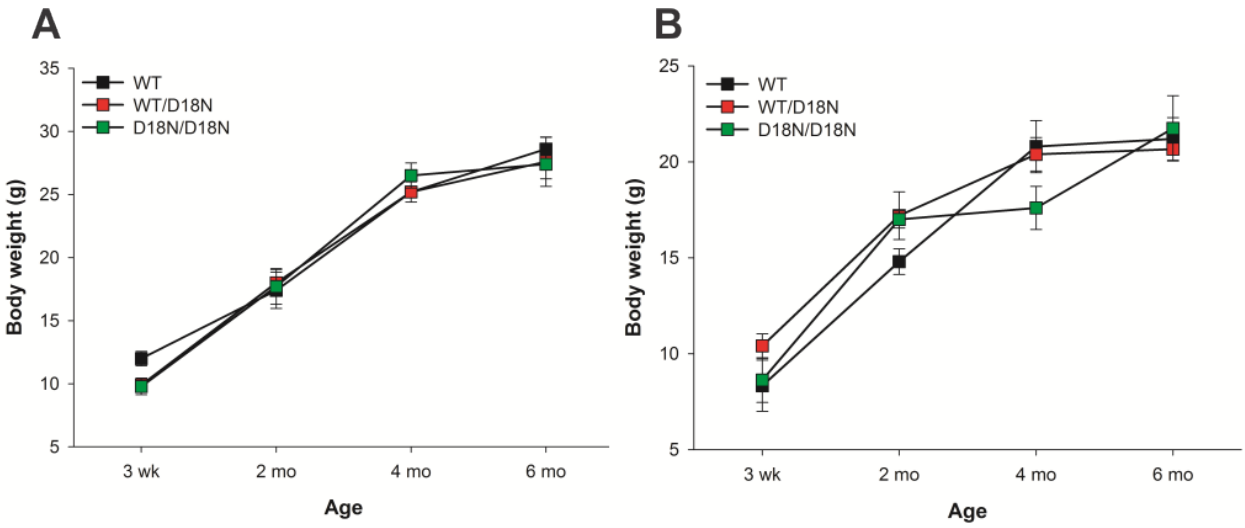

Fig. S6 Growth of *TREX1* mice. (A), Male and **(B)**, female mice were weighed at the time of sacrifice. Data points represent the mean of 3-8 mice. Bars represent the mean and error bars represent s.e.m.

A

Score	Description
0	none
1	Mild proliferation of mesangial cells and/or membrane thickening in <50% of glomeruli
2	Mild proliferation of mesangial cells and/or membrane thickening in >50% of glomeruli
3	Moderate proliferation of mesangial cells and/or membrane thickening in <50% of glomeruli
4	Moderate proliferation of mesangial cells and/or membrane thickening in >50% of glomeruli
5	Severe proliferation of mesangial cells and/or membrane thickening in <50% of glomeruli
6	Severe proliferation of mesangial cells and/or membrane thickening in >50% of glomeruli
7	Severe proliferation of mesangial cells and/or membrane thickening in <50% of glomeruli + glomerulosclerosis in <50% of glomeruli
8	Severe proliferation of mesangial cells and/or membrane thickening in >50% of glomeruli + glomerulosclerosis in >50% of glomeruli

B

Score	Description
0	normal
1	degeneration/regeneration of 1-25% of tubules +/- proteinosis
2	degeneration/regeneration of 26-75% of tubules +/- proteinosis
3	degeneration/regeneration of 76-100% of tubules +/- proteinosis

C

Score	Description
0	None
1	Minimal
2	Mild
3	Moderate
4	Severe
5	Severe with fibrosis

Fig. S7 Histopathology scoring of renal lesions. Kidneys from 8-10 6 mo old mice of each genotype were scored for **(A)**, glomerular lesions; **(B)**, tubular lesions; and **(C)**, inflammation. Scores from were combined to determine the overall score reported in Fig. 2I.

Supplemental Tables

Table S1. Mouse matings

Mating type	Matings	Litters	Pups	Avg # of pups/litter
Trex1$^{WT/WT}$ x *Trex1*$^{WT/WT}$	4	8	46	5.8
Trex1$^{WT/D18N}$ x *Trex1*$^{WT/D18N}$	13	46	211	4.6*
Trex1$^{D18N/D18N}$ x *Trex1*$^{D18N/D18N}$	4	15	68	4.5*

*p<0.05

Table S1. Mouse matings. The pups generated from WT, heterozygous, and homozygous mice were enumerated to determine average litter size.

Table S2. Inflammation Scoring

Score	Description
0	Normal
1	Minimal
2	Mild
3	Moderate
4	Severe
5	Severe with extensive tissue destruction/ necrosis

Table S2. Inflammation scoring. Tissues from 8-10 6 mo old mice of each genotype were scored for inflammation. Each organ received an individual score.

Table S3. Lymphoid Hyperplasia Scoring

Score	Description
0	none
1	mild (follicles mildly enlarged and/or mildly increased number of germinal centers)
2	moderate (follicles moderately enlarged with less distinct zones and/or moderate increase in number of germinal centers)
3	severe (follicles enlarged and coalescing, zones indistinct and/or marked increase in number of germinal centers)

Table S3. Lymphoid hyperplasia scoring. Tissues from 8-10 6 mo old mice of each genotype were scored for lymphoid hyperplasia.

Table S4. Vasculitis Scoring

Score	Description
0	None
1	One vessel
2	Two or more vessels
3	One or more vessels with extensive tissue destruction/ necrosis

Table S4. Vasculitis scoring. Tissues from 8-10 6 mo old mice of each genotype were scored for vasculitis. Tissues were scored individually. A final score was determined by adding scores of all affected tissues.

Table S5. Data collection and refinement statistics (molecular replacement)

	TREX1-D18N:dsDNA
Data collection	
Space group	P21
Cell dimensions	
a, *b*, *c* (Å)	83.1, 84.4, 103.0
α,β,γ (°)	90.0, 102.1, 90.0
Resolution (Å)	20 – 2.8 (2.9 – 2.8)*
R_{merge}	10.2% (43.0%)
Mean I / σ*I*	5.4 (1.2)
Completeness (%)	94.9 (90.5)
Redundancy	3.0 (2.56)
Refinement	
Resolution (Å)	20 - 2.8Å
No. reflections	25822
R_{work} / R_{free}	21.7% / 26.6 %
No. atoms	
Protein	6931
DNA	1698
Mg	4
Wilson B factor	54
Average B-factor	57
Protein atoms B	56
DNA atoms B	62
Mg ions B	39
r.m.s. deviations	
Bond lengths (Å)	.05
Bond angles (°)	1.51

*Values in parentheses are for highest-resolution shell.

References.

1. Lehtinen DA, Harvey S, Mulcahy MJ, Hollis T, & Perrino FW (2008) The TREX1 double-stranded DNA degradation activity is defective in dominant mutations associated with autoimmune disease. *J Biol Chem* 283(46):31649-31656.
2. de Silva U*, et al.* (2007) The crystal structure of TREX1 explains the 3 ' nucleotide specificity and reveals a polyproline II helix for protein partnering. *J. Biol. Chem.* 282(14):10537-10543.
3. Pflugrath JW (1999) The finer things in X-ray diffraction data collection. *Acta Crystallographica Section D-Biological Crystallography* 55:1718-1725.
4. McCoy AJ*, et al.* (2007) Phaser crystallographic software. *Journal of applied crystallography* 40(Pt 4):658-674.
5. Emsley P & Cowtan K (2004) Coot: model-building tools for molecular graphics. *Acta Crystallographica Section D-Biological Crystallography* 60:2126-2132.
6. Murshudov GN, Vagin AA, & Dodson EJ (1997) Refinement of macromolecular structures by the maximum-likelihood method. *Acta Crystallographica Section D-Biological Crystallography* 53:240-255.
7. Adams PD*, et al.* (2002) PHENIX: building new software for automated crystallographic structure determination. *Acta Crystallogr D Biol Crystallogr* 58(Pt 11):1948-1954.
8. Painter J & Merritt EA (2006) Optimal description of a protein structure in terms of multiple groups undergoing TLS motion. *Acta Crystallogr D Biol Crystallogr* 62(Pt 4):439-450.
9. Joosten RP, Long F, Murshudov GN, & Perrakis A (2014) The PDB_REDO server for macromolecular structure model optimization. *IUCrJ* 1(Pt 4):213-220.
10. Perrino FW, Mazur DJ, Ward H, & Harvey S (1999) Exonucleases and the incorporation of aranucleotides into DNA. *Cell Biochem Biophys* 30:331-352.
11. Orebaugh CD*, et al.* (2013) The TREX1 C-terminal region controls cellular localization through ubiquitination. *J Biol Chem* 288(40):28881-28892.